International Journal of Chemical and Biochemical Sciences
(ISSN 2226-9614)

Journal Home page:www.iscientific.org/Journal.html



# Synthesis and Characterization of a new family of borated glasses doped by $V_2O_5$, $P_2O_5$ and $Nb_2O_5$

*Azeddine Elbadaoui[1], Otmane Kharbouch[2], Khadija Dahmani[1],Mouhsine Galai[2*],Mohammed Cherkaoui[1] and Taoufiq Guedira[1]*

[1]*Laboratory of Organic Chemistry, catalysis and Environment, Faculty of Sciences, ibn tofail university, kenitra, Morocco*

[2]*Laboratory of Advanced Materials and Process Engineering, Faculty of Sciences, ibn tofail university, kenitra, Morocco*

**Abstract**

The interest in glasses has prompted new studies of their structure. The absence of order in these materials does not allow them to apply the usual methods of studying the structures of crystalline solids. On the other hand, certain spectroscopic methods are capable of providing important information on the structural units and their arrangement.the novelty of this study is to synthesize and characterize a new borated glasses .The glass series with general formula $Bi_2O_3$-$B_2O_3$ - $M_2O_5$ and $Bi_2O_3$-$B_2O_3$-($Nb_2O_5$- $M_2O_5$) Avec M=P, Ta or V was prepared and characterized by Infrared Spectroscopy (IR)and X-ray Diffraction, the obtained result show that the increase in the contents of Nb2O5 and P2O5 in the Bi2O3-$B_2O_3$- ($Nb_2O_5$-$P_2O_5$) system leads to decrease in the intensity of the band corresponding to the B-O-P groups, the disappearance of the Bi-O-B bands and the disappearance of the bands assigned to the orthoborate and orthophosphate groups. In the other hand, the increase in the contents of $Ta_2O_5$ and $Nb_2O_5$ in the $Bi_2O_3$-$B_2O_3$-($Ta_2O_5$-$Nb_2O_5$) show a disappearance of the band corresponding to the groupings BO3 orthoborates and the disappearance of the inversion of $\upsilon_{as}$ (BO) in $BO_3$.In addition the obtained results show that the vitreous materials of the Bi2O3-B2O3-M2O5 systems are mainly focused on the domain rich in bismuth and boron oxide.

**Keywords:**glasses, Infrared Spectroscopy, X-ray Diffraction, orthophosphate,

**Full length article** **Corresponding Author,* e-mail:galaimouhsine@gmail.com

## 1. Introduction

Many research works have been devoted to glassy materials because of their ease of elaboration and their great utility in various technological fields: optical switches, optical fibers, lasers, ionic conductors, semiconductors, microelectronics, utensils for industry and some domestic uses, etc. Most of the research published so far concerns silicate and borate glasses. With the exception of some so-called "special" glasses, dedicated to optical applications (halide glass for power lasers, chalcogenide glass for infrared transmission). Industrial glasses are made exclusively of oxides and mainly of silica [1-3]. Indeed, $SiO^2$ gives silicate glasses remarkable properties (inalterability, resistance to thermal shocks) and its natural abundance ensures a competitive cost price compared to high quality products. Phosphate glasses have not received as much importance because of the lesser commercial value of the known phases before the last three decades [4,5].

The interest in glasses has led to new studies of their structure. The lack of order in these materials does not allow the application of the usual methods of studying the structure of crystalline solids, but some spectroscopic methods are likely to provide important information on the structural units and their arrangement. Among the most frequently used are infrared and Raman spectroscopies, nuclear magnetic resonance (NMR), paramagnetic resonance (EPR), fine X-ray studies, etc. [6,7].The strong polarizability of the $Bi^{3+}$ ion gives rise to interesting physical properties due to the non-binding 6s2 doublet which is often endowed with stereochemical activity [8]. Many studies have been carried out on oxygenated combinations of bismuth and transition [9-11] or alkali [12] or alkaline earth metals [13], such as, the anionic conductivity in $Bi_2O_3$-(CaO, SrO, PbO, $Y_2O_3$, $Ln_2O_3$....) systems [14,15], Ferroelasticity in $BiVO_4$ [16-18] and the superconducting properties of the Bi-Sr-Cu-O system phases such as $Sr_2Bi_2CuO^{7+}$ ; [19] or of the $Bi_2Sr_{3-x}Ca_xCu_2O_{7+y}$ system [20].

The research envisaged in the context of this work aims to explore the vitreous phases of the ternary diagrams

$Bi_2O_3$-$B_2O_5$-$M_2O_5$ and $Bi_2O_3$-$B_2O_5$-($Nb_2O_5$-$M_2O_5$) with (M=P, V and Ta) in order to evidence of new vitreous materials, the studied glasses was prepared and characterized by Infrared Spectroscopy (IR)and X-ray Diffraction.

## 2. Materials and methods

### *2.1. Initial products*

The different glassy samples were synthesized from ammonium hydrogen phosphate $(NH_4)_2HPO_4$ (Reidel-Hen) and commercial oxides: Niobium oxide $Nb_2O_5$ (fluka), $Bi_2O_3$ oxide (LOBA CHEMIE PVT. LTD.), Boron oxide $B_2O_3$ (fluka), Vanadium oxide $V_2O_5$ (Aldrich), Tantalum oxide $Ta_2O_5$ (fluka).

### *2.2. Synthesis of the glassy phases of the systems $Bi_2O_3$-$B_2O_3$-$M_2O_5$And $Bi_2O_3$-$B_2O_3$-($Nb_2O_5$ -$M_2O_5$) with M= V, Ta or P*

The glassy phases of the systems$Bi_2O_3$-$B_2O_3$-$M_2O_5$ and $BiO_3$-$B_2O_3$-($Nb_2O_5$ -$M_2O_5$) with (M= P, Ta or V) are obtained by melting stoichiometric mixtures of the starting products according to the reaction scheme:

- **System $Bi_2O_3$-$B_2O_3$ -$P_2O_5$**

(1-x-y)$Bi_2O_3$+x$B_2O_3$+y$(NH_4)_2HPO_4$→ (1-x-y) $Bi_2O_3$ + x$B_2O_3$ + y/2$P_2O_5$ +2y$NH_3$+y/2$H_2O$

1-x-y, x and y are respectively the molar fractions of $Bi_2O_3$, $B_2O_3$, $P_2O_5$.

- **System $Bi_2O_3$-$B_2O_3$ -$V_2O_5$**

(1-x-y)$Bi_2O_3$+x$B_2O_3$+y$V_2O_5$→ (1-x-y) $Bi_2O_3$+x$B_2O_3$+ y$V_2O_5$

1-x-y, x and y are respectively the molar fractions of $Bi_2O_3$, $B_2O_3$, $V_2O_5$.

- **System $Bi_2O_3$-$B_2O_3$ -$Ta_2O_5$**

(1-x-y)$Bi_2O_3$+x$B_2O_3$+y$Ta_2O_5$→ (1-x-y) $Bi_2O_3$+x$B_2O_3$+ y$Ta_2O_5$

1-x-y, x and y are respectively the molar fractions of $Bi_2O_3$, $B_2O_3$, $Ta_2O_5$.

- **System $Bi_2O_3$-$B_2O_3$-(50%$Nb_2O_5$ –50%$P_2O_5$)**

(1-x-y)$Bi_2O_3$+x$B_2O_3$+y /2$Nb_2O_5$+y$(NH_4)_2HPO_4$→(1-x-y)$Bi_2O_3$+x$B_2O_3$+y/2$Nb_2O_5$+y/2$P_2O_5$ +2y$NH_3$+y/2$H_2O$

1-x-y, x and y/2 are the molar fractions of $Bi_2O_3$, $B_2O_3$, $Nb_2O_5$and $P_2O_5$ respectively.

- **System $Bi_2O_3$-$B_2O_3$-(50%$Nb_2O_5$ –50%$V_2O_5$)**

(1-x-y)$Bi_2O_3$+x$B_2O_3$+y/2$Nb_2O_5$ + y/2$V_2O_5$ → (1-x-y) $Bi_2O_3$+x$B_2O_3$+ y/2$Nb_2O_5$ + y/2$V_2O_5$

1-x-y, x and y/2 are the molar fractions of $Bi_2O_3$, $B_2O_3$, Nb2O5and $V_2O_5$ respectively.

- **Système $Bi_2O_3$-$B_2O_3$-(50%$_{Nb2O5}$ –50%$Ta_2O_5$)**

(1-x-y)$Bi_2O_3$+x$B_2O_3$+y/2$Nb_2O_5$ + y/2$Ta_2O_5$ → (1-x-y) $Bi_2O_3$+x$B_2O_3$+ y/2$Nb_2O_5$ + y/2$Ta_2O_5$

1-x-y, x and y/2 are the molar fractions of Bi2O3, B2O3, Nb2O5 and $Ta_2O_5$ respectively.

The reagents are intimately ground in an agate mortar and then introduced into alumina crucibles or gold pods.A first heat treatment was performed at 350°C for one night followed by grinding,in order to complete the total decomposition of the ammonium hydrogen phosphate.Then the temperature was increased in steps of 50°C to avoid chemical losses by volatilization.The reaction mixture is then brought to a temperature above the melting temperature.The molten mixture is then dipped in the open air in an alumina mold previously heated to about 200°C.

## 3. Results and discussion

Purely amorphous samples are always synthesized as a translucent mass.When the quenched liquid gives rise to a glass-ceramic mixture, the materials obtained become less and less translucent as one moves away from the limit of the glassy domain.X-ray diffraction allowed us to identify the vitrifiable compositions within the examined system.Indeed, any sample whose X-ray diffractogram did not contain diffraction lines was considered as belonging to the glassy system. Thus we have delimited the glassy domains within the ternaries.

### *3.1 Delimitation of the glassy domains within the ternary $Bi_2O_3$-$B_2O_3$-(1-x)$P_2O_5$-x$Nb_2O_5$*

Figure 1 represents the waxy domain corresponding to compositions containing only Phosphorus and the delimitation of the glassy domain within the $Bi_2O_3$-$B_2O_3$-(0.5$P_2O_5$-0.5$Nb_2O_5$) ternary,Figure2 allows us to evaluate the extent of each domain in relation to the other.We observe that increasing the Niobium content increases the extent of the glassy domain.We can notice that the phosphorus intervenes strongly in the depolymerization of the vitreous framework from where the domain more restricted that present the phases of this one in comparison with those of the niobium and the Phosphorus.

It should be noted that the preparation conditions such as the quenching speed, the total mass of the sample, the nature of the products to be vitrified, the duration and the temperature of the treatment are considered among the most important factors in the variation of the limits of these glassy phases.

### *3.2 Delineation of the glassy domains within the ternary $Bi_2O_3$-$B_2O_3$-(1-x)$V_2O_5$-x$Nb_2O_5$)*

Figures 3and 4 represent respectively the glassy zones delimited within the ternary diagrams $Bi_2O_3$-$B_2O_3$-(1-x)$V_2O_5$-xNb with x=0 and x=0.5.We can point out that vanadium is strongly involved in the depolymerization of the glass framework hence the narrower range of its phases compared to those of niobium and vanadium.

### *3.3. Delimitation of the glassy domains within the ternary $Bi_2O_3$-$B_2O_3$-(1-x)$Ta_2O_5$-x$Nb_2O_5$*

Figures 5and 6 represent respectively the glassy zones delimited within the ternary diagrams $Bi_2O_3$-$B_2O_3$-(1-x)$Ta_2O_5$-xNb with x=0 and x=0.5.We can point out that tantalum is strongly involved in the depolymerization of the glass framework, hence the more restricted range of its phases compared to those of niobium and tantalum.

Subsequently we studied three axes of glassy systems in this work:

- Axis : (0.90-x) $Bi_2O_3$-x$B_2O_3$-0,1$M_2O_5$ avec 0.3≤ x ≤0.5
- Axis :(0.95-x) $Bi_2O_3$-x$B_2O_3$-(0,025$M_2O_5$-0,025$Nb_2O_5$) avec 0.3≤ x ≤0.5
- Axis : (0.90-x) $Bi_2O_3$-x$B_2O_3$-(0,5$M_2O_5$-0,5$Nb_2O_5$) avec 0.3≤ x ≤0.5.

Such as M=P, V or Ta.

### *3.3.1 X-ray diffraction*

We have chosen to study the system (0.90-x)$Bi_2O_3$-x$B_2O_3$-0,1$P_2O_5$ by ray diffraction to verify that it is an amorphous phase,Figure7 represents the diagrams obtained for the different values of x,Figures 8 to 11 show the spectra obtained from the point in the middle of each axis studied.he X-ray spectra do not show any Bragg peaks. The absence of diffraction and the presence of bumps are consistent with the amorphous state of all glassy systems studied.

### *3.3.2 Study by infrared vibration spectroscopy*

#### *3.3.2.1 Role of vibrational spectroscopy in the approach of glassy structures.*

The vibrational spectroscopy in the Infrared and Raman approach allows reaching a wider spatial domain, since they address the vibrations of entities (molecules or polyatomic groups) constituting the amorphous material, unlike other spectroscopic methods (NMR, EXAFS, EPR ….) Thanks to the analysis of the vibration spectrum, it is possible in many cases, to approach the short-range structure of amorphous compounds.The interaction of vibrational spectra requires knowledge of the rules of group theory that use the symmetry properties of molecules and crystals. This theory is a powerful tool in the case of crystallized materials ordered over the entire extent of their three-dimensional network, but its scope in the case of amorphous materials is more limited because the order exists only at short distances. In the glassy state, as in the crystalline state, the molecules or group of atoms are not isolated. These entities are in strong interaction with each other. In a glassy sample, an elementary mesh cannot be defined and the whole sample must be considered as a single mesh containing a giant molecule with an infinity of vibrating entities, which leads to a widening of the bands. On the other hand, there is a way to check if we have a crystalline or amorphous phase such that the vibrational spectrum of a crystallized sample presents fine and well resolved bands.

#### *3.3.2.2.Studies of glasses of composition (0.90-x) $Bi_2O_3$-x$B_2O_3$-0.1$P_2O_5$*

Considering a constant level of phosphorus (x=0.1), figures 12 and 13 show the infrared absorption and Raman scattering spectra, Table 2 groups the different attributions of the frequencies observed in the infrared and RAMAN spectra of the compound glasses:

(0,90-x) $Bi_2O_3$-x$B_2O_3$-0,1$P_2O_5$

The vibration between 420-490 cm-1 has several attributions. It is an overlap of the bands of different structural units.It is attributed to the vibration of the B-O-B bond in the borate units in pure $B_2O_3$ glasses [22,23].It may also have its origin from the vibration of Bi-O-Bi bonds [24].The six-membered rings containing one or two boron atoms in coordination IV are responsible for the appearance of the band between 500-540$cm^{-1}$[25,26].The vibration of the chain and/or cyclic units of the metaborate type appears between 600-690$cm^{-1}$[27,28], corresponding to the vibration of the B-O-P bond in the MB (and/or MB') type entities of alkali borophosphate glasses [29-30].By analogy, this band can be attributed to borophosphate groups formed by isolated $O_2PO^-_{2/2}$ metaphosphate entities linked to metaborate units.The vibration at 970$cm^{-1}$ is attributed to six-membered borate rings containing one or two boron atoms in coordination IV [31,32].The bands around 1000$^{-1}$ -1100 $cm^{-1}$are attributed to O-P-O vibrations in the MB and/or MB' units [33,34]. The absence of any band corresponding to the P=O group in our spectrum [23],eliminates the hypothesis of the presence of isolated $PO_4$ groups, which clearly indicates the formation of central units of MB' type only, in which the $PO_4$ tetrahedra contain two bridging oxygens each.We can therefore suggest that the broad band is composed, either attributed to borophosphate units of type $MB'_1$ $MB'_2$ linked to diborate units in accordance with the study by Belfaquir et al [21].The band between 1190-1240$cm^{-1}$ is attributed to the vibration of $B\text{-}O^-$ end groups in pyroborate units [28, 31,36].The vibration around 1270-1310 cm-1 is attributed to the asymmetric B-O elongation mode in the orthoborate ($BO_3$) units.The progressive addition of $B_2O_3$ causes an increase in the intensity of the bands located around 420-490 ,500-540,600-690 $cm^{-1}$ and the decrease in the intensity of the band around 1190-1240 $cm^{-1}$. The broad band located around 980-1000 $cm^{-1}$ is dominant.The decrease of the line intensity around 1190-1240$cm^{-1}$ assigned to pyroborate units compared to that around 600-690 $cm^{-1}$ for metaborate units is explained by the conversion of pyroborate units into metaborate units.
However, the decrease in the intensity of the band attributed to pyroborates compared to the broad band around 980-1000$cm^{-1}$ seems to be related to the conversion of pyroborates into diborate entities. This transformation is probably related to the increase of the rate of bores atoms of coordinacyIV[37].

### *3.4. Study of glasses of the composition (0.90-x)$Bi_2O_3$-x$B_2O_3$-(0.05$P_2O_5$-0.05$Nb_2O_5$)*

Table 1 gives the molar fractions corresponding tothe system (0,90-x)$Bi_2O_3$-x$B_2O_3$-(0,05$P_2O_5$-0,05$Nb_2O_5$). Figure 14 represents the infrared spectra of this system. Thefrequencies and their attributions are gathered in table 1. Figure 14 and Table 3 represent the infrared spectra and their attributions. Examination of these spectra shows that the substitution of bismuth by boron results in a decrease in the intensity of the Bi-O-Bi moiety and an increase in the intensity of B-O-B.We also notice a shift of the characteristic bands at metaborate units towards the highfrequencies.The pyroborate units appear with intensity for high boron content, however the decrease in intensity of the band attributed to BO ($B_4^-$) seems to be explained by the conversion of this grouping into $BO^-$ units in the pyroborate.

### 3.5. Studies of glasses of composition (0.95-x) $Bi_2O_3$-x $B_2O_3$-(0.025 $P_2O_5$-0.025 $Nb_2O_5$).

Table 4 gives the corresponding mole fractions (0.95-x)$Bi_2O_3$-x$B_2O_3$-(0.025$P_2O_5$-0.025$Nb_2O_5$). Figure 15 represents the infrared spectra of this composition.The frequencies and their assignments are recorded in Table 5.Table 5 gathers the frequencies and the assignments of the infrared bands. The examination of these spectra shows that the substitution of bismuth by boron leads to an increase in the intensity of the bands assigned to the B-O-Bi and B-O-B groups and a decrease in the intensities of the Bi-O-Bi bands.We observe an increase in the intensity of the band assigned to the B-O-P units and the υas (BO) vibration in ($BO_3$). On the other hand we observe a decrease in the bands assigned to the pyroborate units.The evolution of these bands seems to be explained by the conversion of pyroborate units into metaborate units.We also notice the disappearance of orthophosphate and boroxol units, which can be explained by the conversion of orthophosphate and boroxol units into orthoborate and BO- units in the pyroborate.

### 3.6. Studies of glasses of composition (0.90-x)$Bi_2O_3$-x$B_2O_3$ -0.1$V_2O_5$

Figure 16 and Table 6 correspond to the Raman and infrared spectra for constant vanadium levels, respectively.
The Raman spectra confirm the non-existence of the band at 1050$cm^{-1}$ and the presence of the 880 $cm^{-1}$ band for all compositions. The hypothesis of the presence of MB2 and MB'2 groups seems to us the most probable.The infrared spectra show the presence of metaborates and diborates in the glass frameworks, bands at 1320 $cm^{-1}$ and 1220 $cm^{-1}$ respectively. However, the bands with boron in the four coordinates are intense in the case of compositions containing only vanadium.

### 3.7. Study of glasses of the composition (0.90-x) $Bi_2O_3$-x $B_2O_3$-(0.05$V_2O_5$-0.05$Nb_2O_5$)

Table 7 gives the molar fractions corresponding to the system(0,90-x)$Bi_2O_3$-x$B_2O_3$-(0,05$V_2O_5$-0,05$Nb_2O_5$). Figure 17 represents the infrared spectra of this composition. The observed bands and their attributions are gathered in table 8.The analysis of the infrared spectra of glasses of compositions(0.90-x) $Bi_2O_3$-x $B_2O_3$-(0.05$V_2O_5$-0.05 $Nb_2O_5$)shows that the substitution of bismuth by boron leads to an increase in the intensities of the bands assigned to the B-O-V metaborate units.We also observe the disappearance of the bands between 770 $cm^{-1}$and 790$cm^{-1}$ attributed to the pyrovanadate groups $V_2O_7^{4-}$ and $VO_4$.We also notice a disappearance of the pyroborate groups B-$O^-$. This can be explained by the conversion of pyroborate units into metaborate units.For a high boron content there is a decrease in the intensity of orthovanadate units. This evolution can be explained by the conversion of orthovanadates into B-O-V metaborate units.

### 3.8. Study of the glasses of the composition (0.95-x) $Bi_2O_3$-x $B_2O_3$-(0.025$V_2O_5$-0.025$Nb_2O_5$)

The Table 9 gives the corresponding molar fractions (0,95-x)$Bi_2O_3$-x$B_2O_3$-(0,025$V_2O_5$-0,025$Nb_2O_5$). Figure 18 represents the infrared spectra of this system. The frequencies and their assignments are recorded in table 9.The analysis of the infrared spectra of glasses of compositions(0.90-x)$Bi_2O_3$-x$B_2O_3$-(0.05$Ta_2O_5$-0.05$Nb_2O_5$)shows that the substitution of bismuth by boron leads to an increase of the intensities of the bands assigned to the metaborate units B-O-Bi and Bi-O-Bi.We also observe the disappearance of the υas(BO) inversion in $BO_3$.We also notice a disappearance of the orthoborate groups $BO_3$.This can be explained by the conversion of orthoborate units into metaborate units.

### 3.9. Study of glasses with compositions (0.95-x)$Bi_2O_3$-x$B_2O_3$-(0.025$Ta_2O_5$-0.025$Nb_2O_5$)

Table 10 gives the corresponding mole fractions. Figure 18 represents the infrared spectra of these compositions. The frequencies and their attributions are collected in table 10.In general, in the range of 600 to 950 $cm^{-1}$ the Nb-O stretching vibrations are observed [35]. The IR band near 920 $cm^{-1}$ is attributed to the stretching mode of the Nb-O bonds, while the stronger one near 620 $cm^{-1}$, has been attributed to the stretching of the deformed Nb-O-Nb bonds in the $NbO_6$octahedra[36].In particular in the region of 500-700 cm-1 (the valence vibration region of Ta-O-Nb (The bridge bonds) [38].The band between 640-650 cm-1 corresponds to the vibration of the Ta-O bond and the 870 cm-1 band is attributed to the vibration of the Ta-O-Ta bond [34].The substitution of bismuth by boron leads to an increase in the intensities of the B-O-Bi bands and a decrease in the intensities of the Bi-O-Bi bands.We notice a disappearance of the band corresponding to the orthoniobate groups υs(Nb-O-Nb).We also observe a shift of the bands assigned to the metaborate groups towards the low frequencies.

### 3.10. Study of density and molar volume

The volume VM, of each composition was evaluated from its density "ρ" and its molar mass
M: VM= M/ρ,
With M= $xM_{Bi2O3}$ + $yM_{B2O3}$+ $zM_{Nb2O5}$ +t$M_{M'2O5}$ with M'= P, V or Ta. $M_{Bi2O3,}$ $MB_{2O3}$, $M_{Nb2O5}$and $M_{M'2O5}$ are respectively the molar masses of Bi2O3, B2O3, Nb2O5and $M'_2O_5$withM'= P, V or Ta.

Figures 18, 19 and 20 show the variations of the density and molar mass of the compositions (0.90-x) $Bi_2O_3$-x$B_2O_3$-(0.05$M_2O_5$-0.05$Nb_2O_5$)with M= P, V or Ta.The rates of the oxides of $M'_2O_5$ with M'= P, V, Ta and Nb are constant; the substitution is made between the bismuth oxide and the boron oxide, figures 19, 20 and 21 shows this variation. We notice the effect of the molar mass prevails, in fact $MBi_2O_3$>>$MB_2O_3$, consequently, we have a decrease of the two quantities, therefore all the curves are descending.

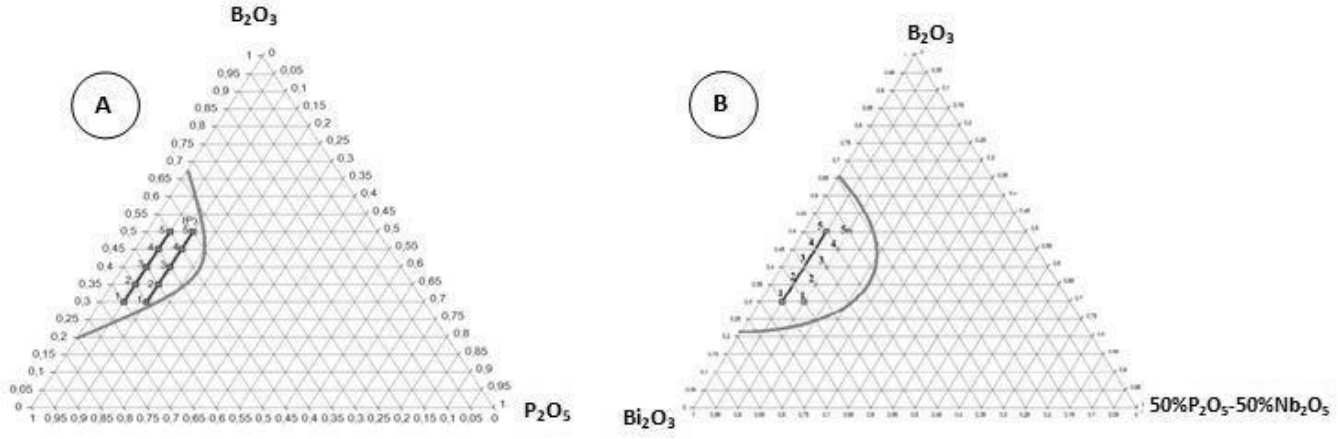


**Figure 1:** Extent of the glassy domain within the ternary system **A=**$Bi_2O_3$-$B_2O_3$-$P_2O_5$ and B= $Bi_2O_3$-$B_2O_3$-(0,5$P_2O_5$-0,5$Nb_2O_5$).

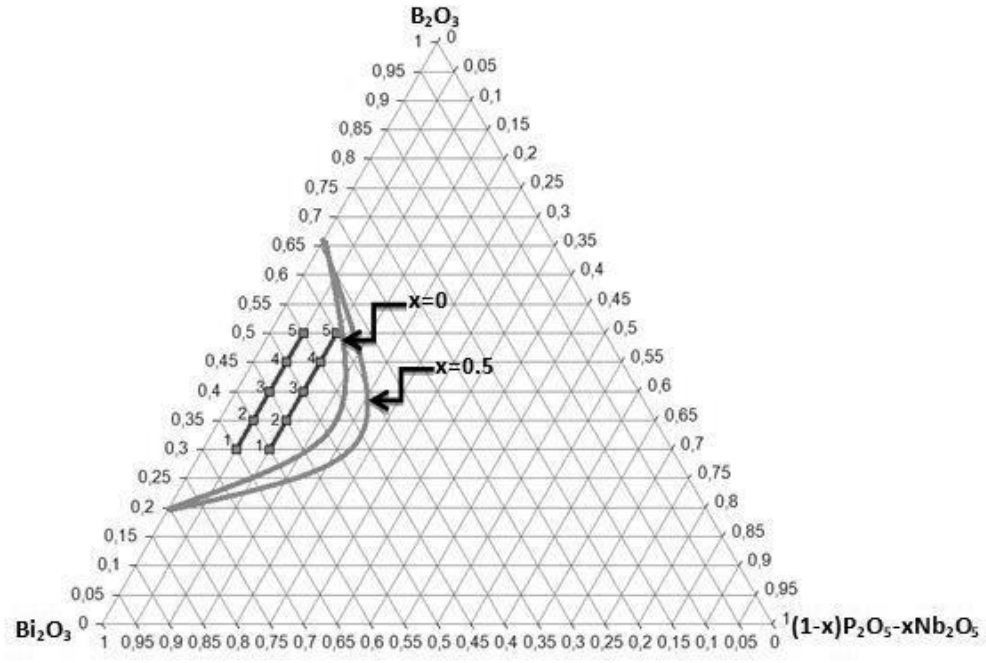


**Figure 2:** Extent of the glassy domain within the ternary $Bi_2O_3$-$B_2O_3$-(1-x)$P_2O_5$-x$Nb_2O_5$

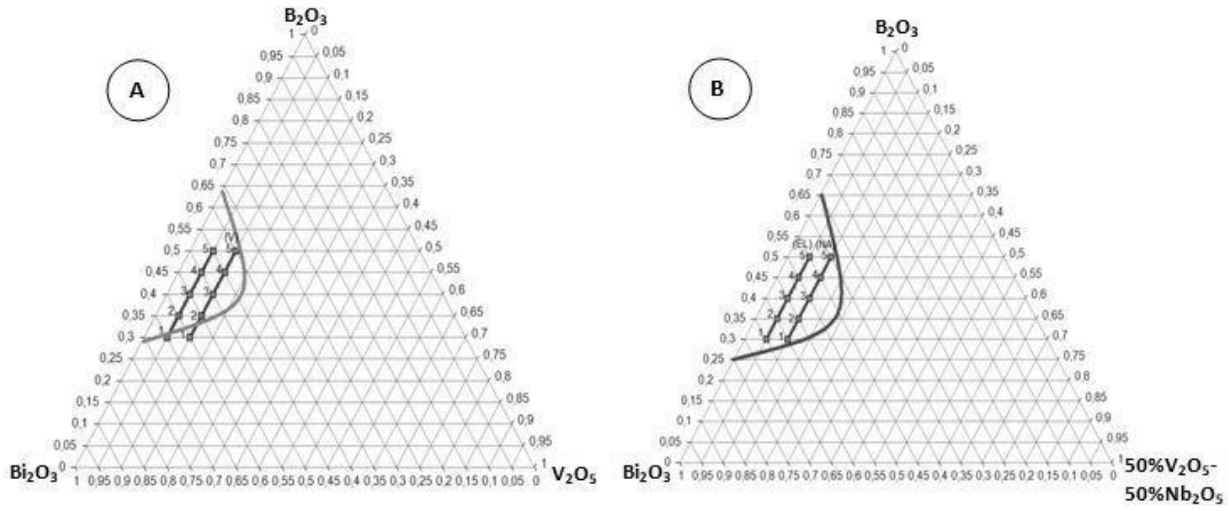


**Figure 3:** Extent of the glassy domain within the ternary system
**A=**$Bi_2O_3$-$B_2O_3$-$V_2O_5$ and **B=**$Bi_2O_3$-$B_2O_3$-(0,5$V_2O_5$-0,5$Nb_2O_5$)

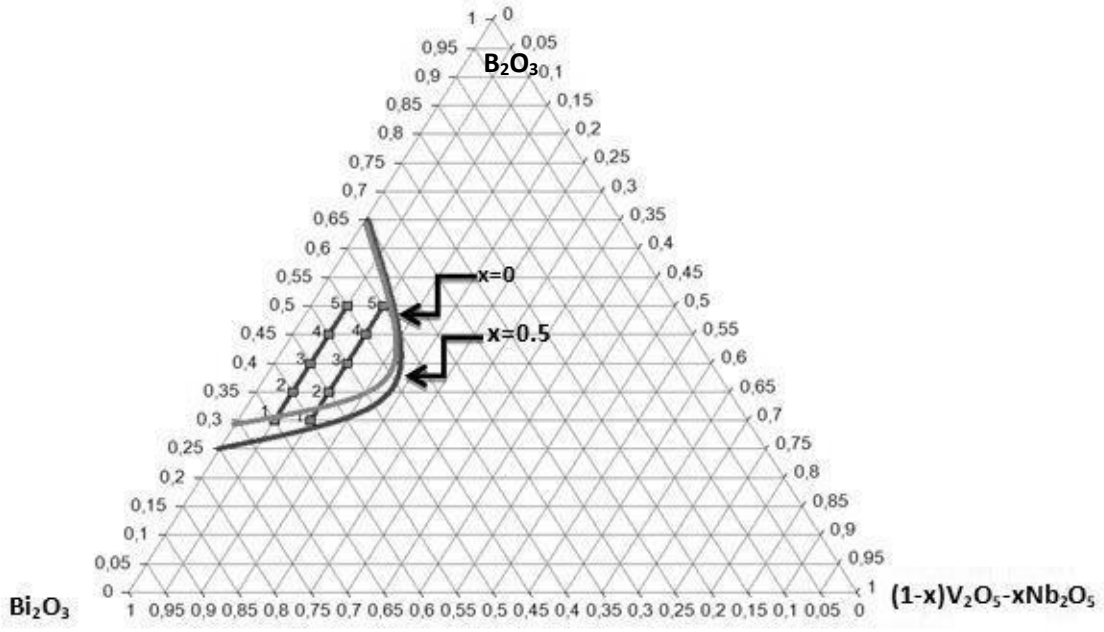


**Figure 4:** Extent of the glassy domain within the ternary$Bi_2O_3$-$B_2O_3$-(1-x)$V_2O_5$-x$Nb_2O$

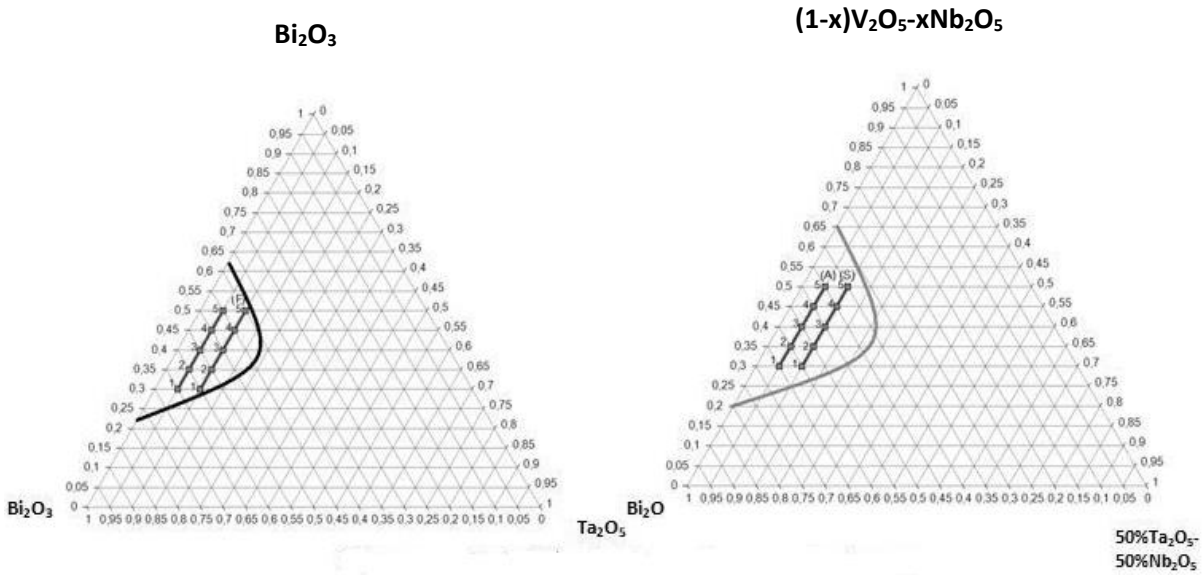


**Figure 5:** Extent of the glassy domain within the ternary
A= $Bi_2O_3$-$B_2O_3$-$Ta_2O_5$ and B= $Bi_2O_3$-$B_2O_3$-(0,5 $Ta_2O_5$-0,5$Nb_2O_5$)

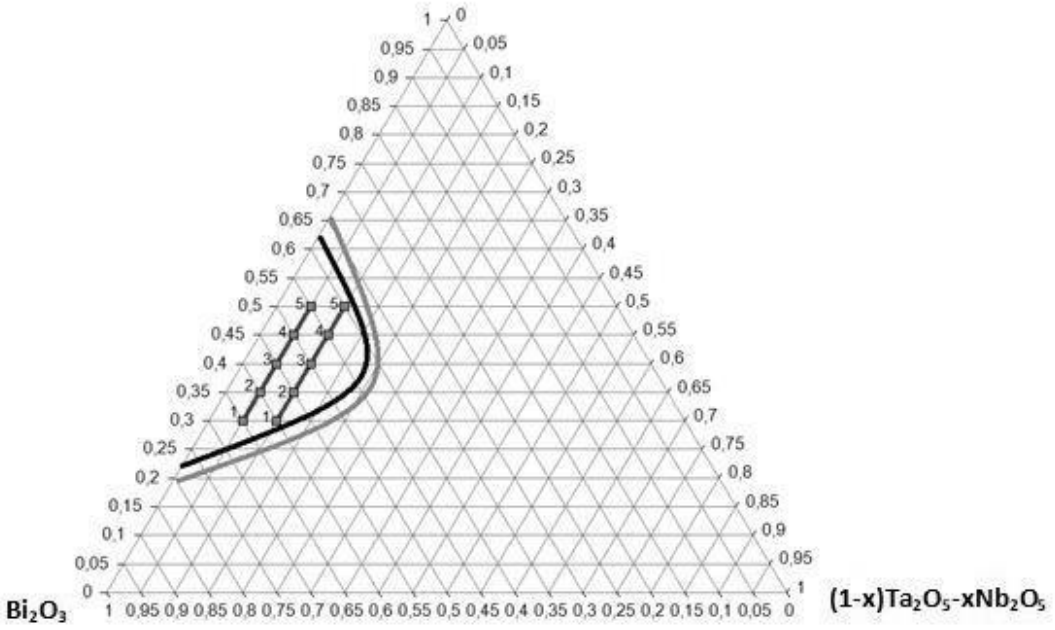


**Figure 6:** Extent of the glassy domain within the ternary
$Bi_2O_3$-$B_2O_3$-(1-x) $Ta_2O_5$-x$Nb_2O_5$

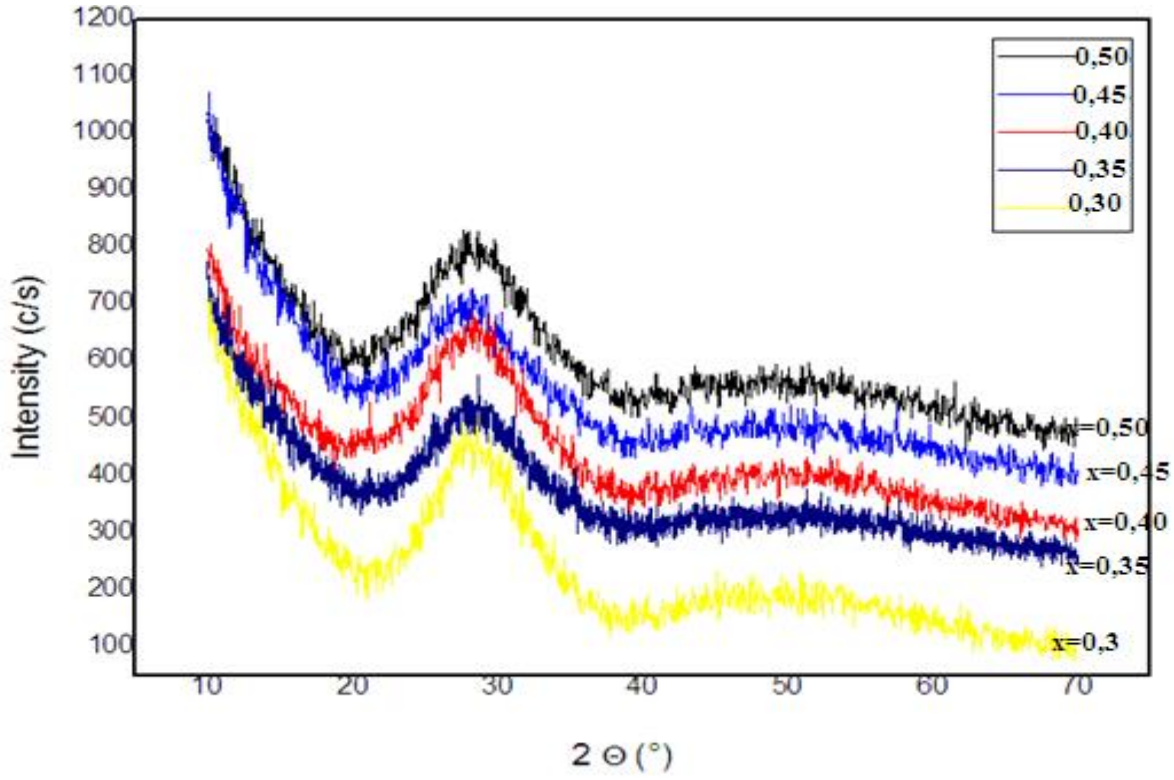


**Figure 7:** X-ray spectra of the system (0.90-x) $Bi_2O_3$-x$B_2O_3$-0.1$P_2O_5$

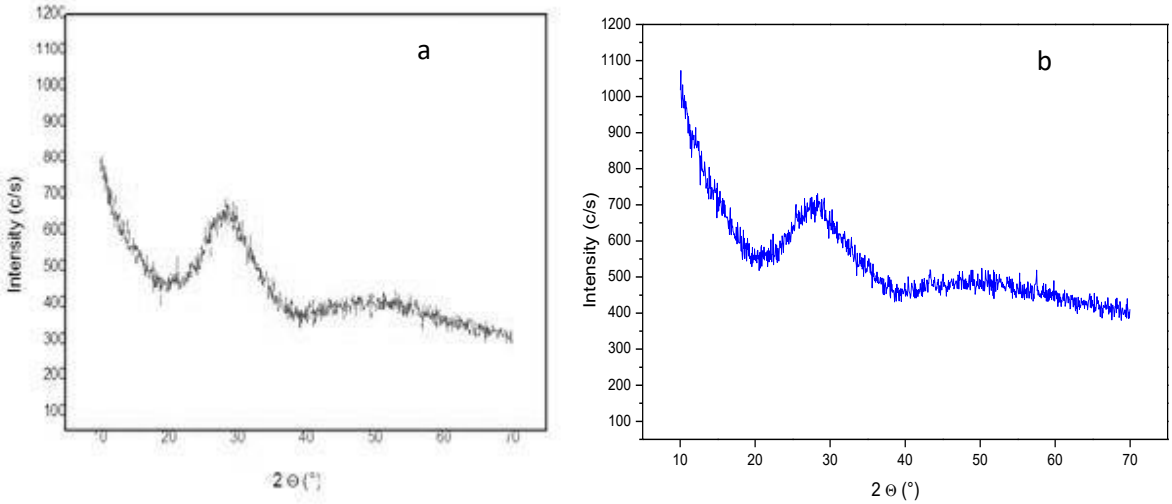


**Figure 8:** X-ray spectrum of the system (a) 0.5$Bi_2O_3$-0.4 $B_2O_3$-0.1$P_2O_5$ and(b) 0.5$Bi_2O_3$-0.4$B_2O_3$-(0.05$Nb_2O_5$-0.05$P_2O_5$)

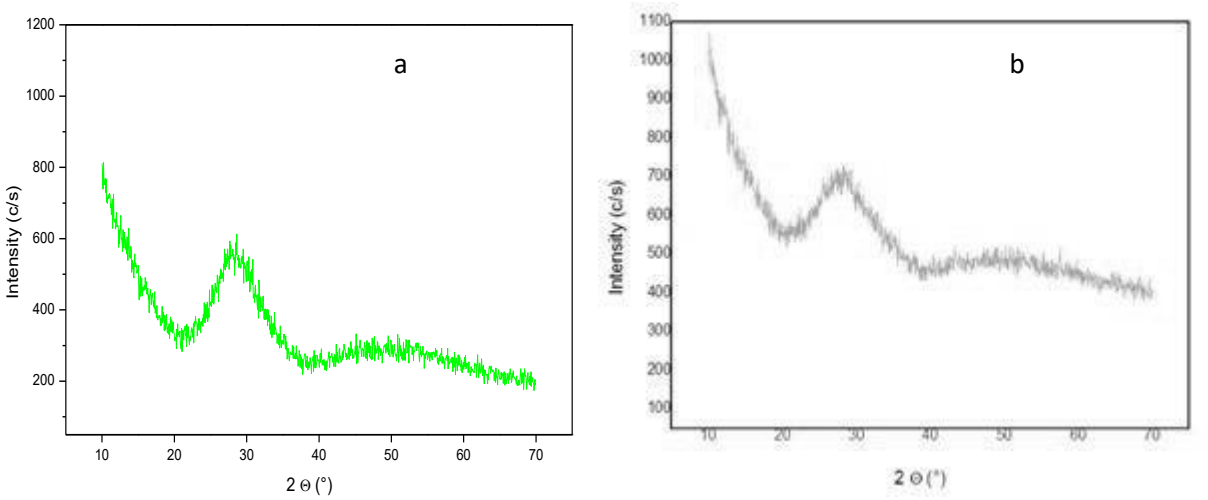


**Figure 9:** X-ray spectrum of the system (a) $0.5Bi_2O_3$-$0.4B_2O_3$-($0.025Nb_2O_5$-$0.025P_2O_5$) and (b) 0,5 $Bi_2O_3$-$0,4B_2O_3$-$0,1V_2O_5$

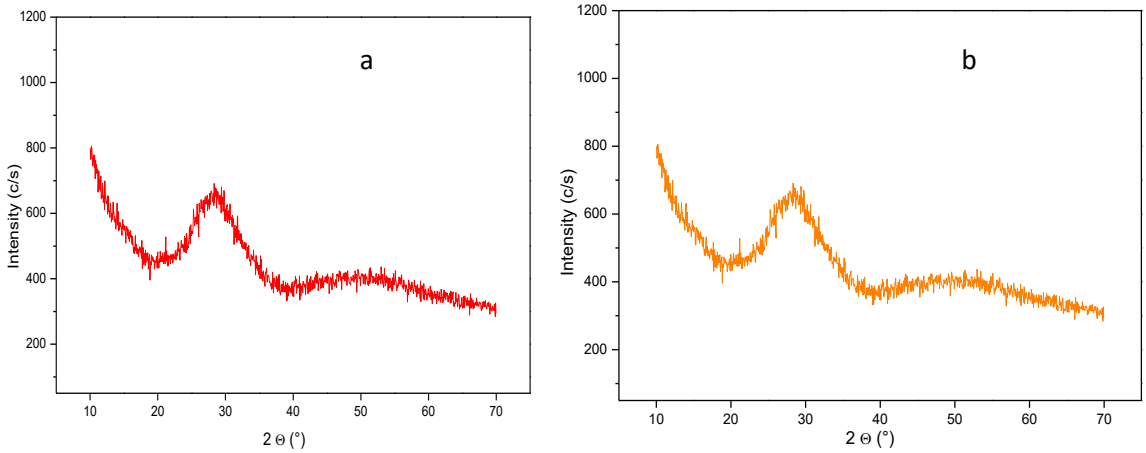


**Figure 10:**X-ray spectrum of the system (a)

$0,5Bi_2O_3$-$0,4B_2O_3$-($0,05Nb_2O_5$-$0,05V_2O_5$) and (b) $0,5Bi_2O_3$-$0,4B_2O_3$-($0,025Nb_2O_5$- $0,025V_2O_5$)

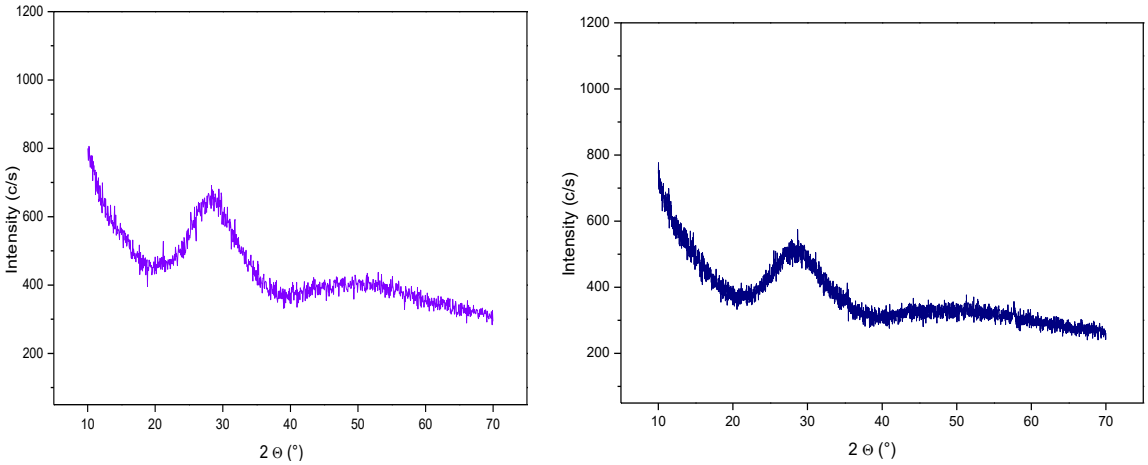


**Figure 11:** X-ray spectrum of the system (a) $0,5Bi_2O_3$-$0,4B_2O_3$-$0,1Ta_2O_5$ and(b) $0,5Bi_2O_3$-0,4 $B_2O_3$-($0,025Nb_2O_5$-$0,025Ta_2O_5$)

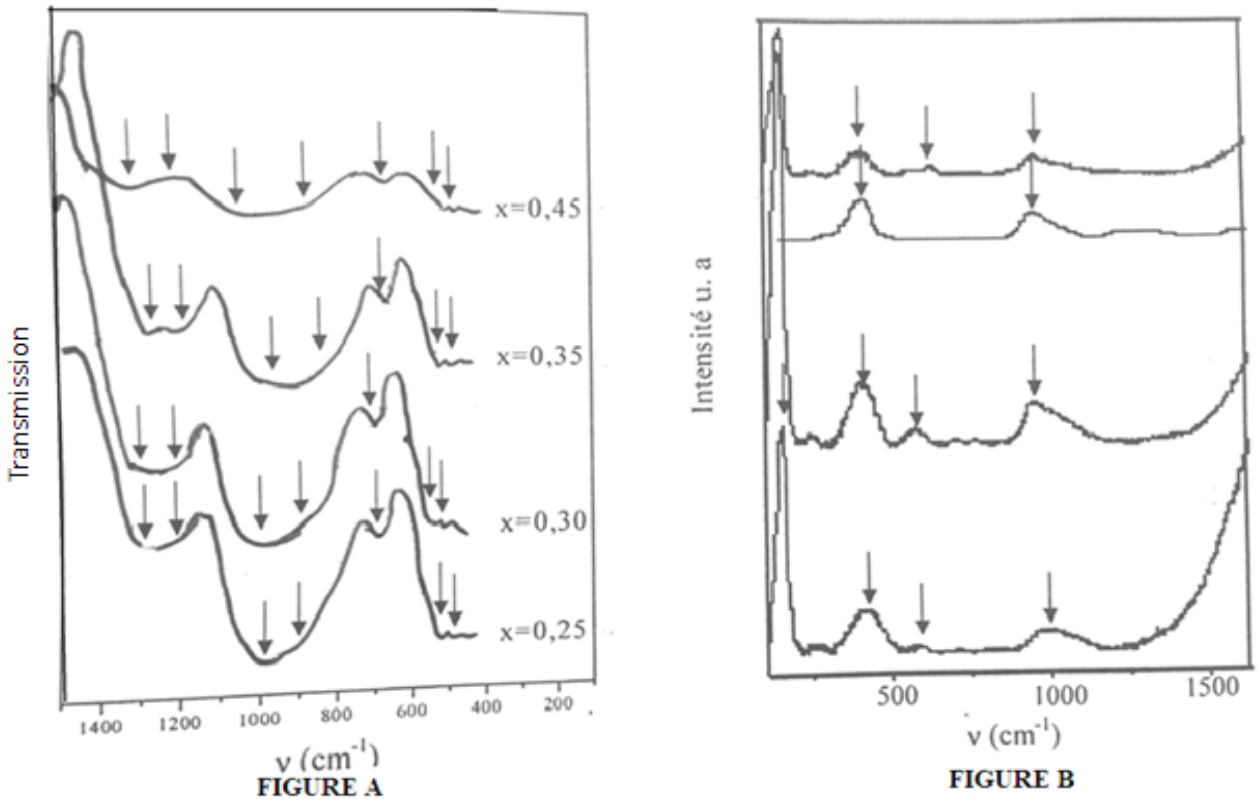


**Figure 12:** Infrared (A) and Raman (B) spectra of glasses of composition$(0,90-x)Bi_2O_3$-$xB_2O_3$-$0,1P_2O_5$

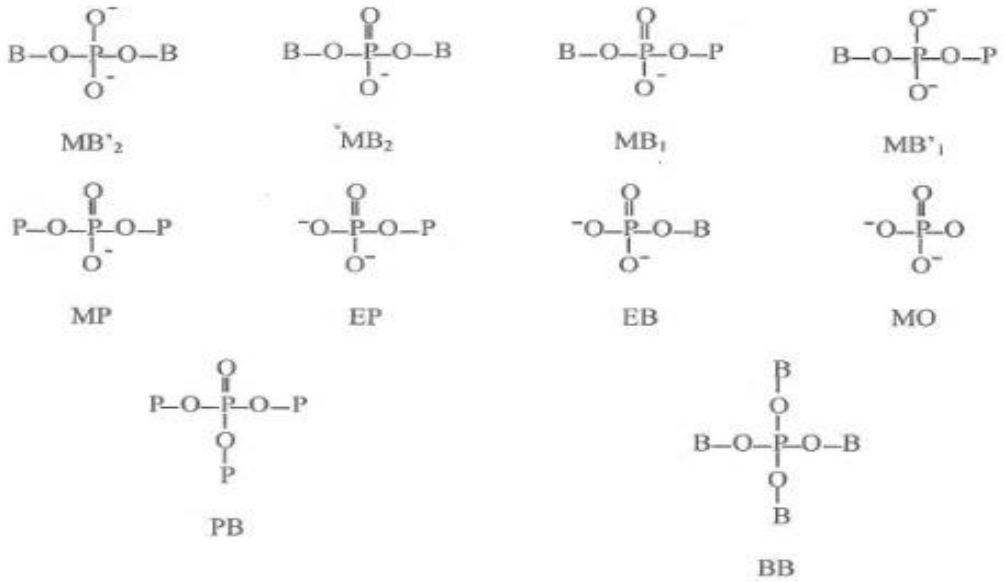


**Figure13:** the positions and attributions of the different vibration modes [21].

**Table 1:** Infrared frequency allocations of the composition glasses(0,90-x)$Bi_2O_3$-x$B_2O_3$-0,1$P_2O_5$

| **Nº ofsample** | | **P1** | | **P2** | | **PP3** | | **P4** | |
|---|---|---|---|---|---|---|---|---|---|
| **Composition** | | **X=0,25** | | **X=0,30** | | **X=0,35** | | **X=0,45** | |
| **Spectroscopy** | | **IR** | **Ra** | **IR** | **Ra** | **IR** | **Ra** | **IR** | **Ra** |
| **Assignments** | **-network vibration δ (B-O-B)** | | 160 | | 160 | | 160 | | 160 |
| | **- vibration Bi-O-Bi in ($BiO_6$)** | | 420 | | 425 | | 436 | | 440 |
| | **- δskeleton Or δ (Bi-O-Bi) Or δ (Bi-O-B)** | 470 | | 490 | | 480 | | | |
| | **-Six-membered rings containing one or two boron atoms in coordination VI** | 520 | | 540 | | 520 | | 500 | |
| | **-metaborate$\nu_2$ (B-O-P)** | 680 | 598 | 690 | 610 | 670 | | 650 | 675 |
| | **-orthophosphate** | 920 | | 910 | | 900 | | 900 | |
| | **-orthoborate ($BO_3$)** | 990 | 980 | 1010 | 970 | 1000 | 965 | 1030 | 970 |
| | **-pyroborates B-$O^-$** | 1240 | | 1230 | | 1190 | | 1220 | |
| | **-$\nu_{as}$(BO) in $BO_3$** | 1290 | | 1310 | | 1270 | | 1300 | |

**Table 2:** Compositions of the samples prepared in the system(0,90-x) $Bi_2O_3$-x$B_2O_3$-(0,05$P_2O_5$-0,05$Nb_2O_5$).

| **Sample** | **X** | **0.90-x** |
|---|---|---|
| **AZ1** | 0.30 | 0.60 |
| **AZ2** | 0.35 | 0.55 |
| **AZ3** | 0.40 | 0.50 |
| **AZ4** | 0.45 | 0.45 |
| **AZ5** | 0.50 | 0.40 |

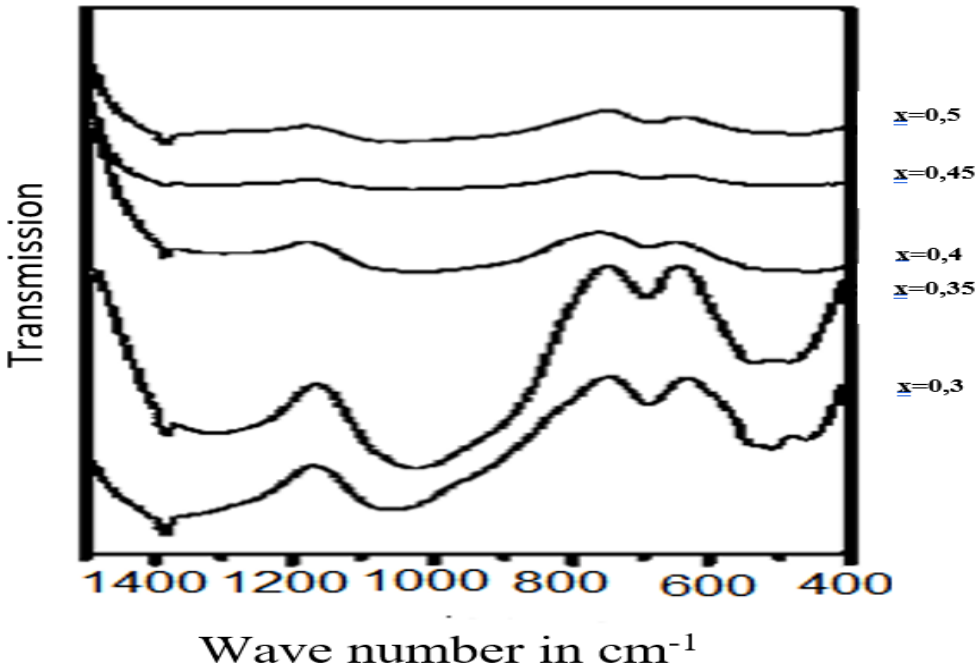


**Figure 14:** infrared spectrum of glass compositions$(0,90-x)Bi_2O_3$-$xB_2O_3$-$(0,05P_2O_5$-$0,05Nb_2O_5)$

**Table 3:** Infrared frequency allocations for glass compositions$(0,90-x)Bi_2O_3$-x $B_2O_3$-$(0,05P_2O_5$-$0,05Nb_2O_5)$

| **Nº ofsample** | **$AZ_1$** | **$AZ_2$** | **$AZ_3$** | **$AZ_4$** | **$AZ_5$** |
|---|---|---|---|---|---|
| **Composition** | **x=0.30** | **x=0.35** | **x=0.4** | **x=0.45** | **x=0.5** |
| **skeleton Bi-O-Bi**<br>**Or skeleton B-O-Bi**<br>**Orskeleton B-O-B** | 478<br>-------<br>537 | 468<br>515<br>533 | 459<br>497<br>542 | 460<br>484<br>500 | 460<br>508<br>536 |
| **Métaborates$\upsilon_{a\ B\text{-}O\text{-}Nb}$** | 654 | 670 | 670 | 671 | -------- |
| **Métaborates$\upsilon_{a\ B\text{-}O\text{-}P}$** | 692 | 692 | 693 | 691 | 687 |
| **Boroxol** | 884 | 896 | 891 | 894 | |
| **BO ($BO^{4-}$)** | 1025 | 1034 | 1068 | 1027 | 1037 |
| **Pyroborates $B\text{-}O^-$** | 1291 | 1290 | 1264 | ---------- | ---------- |
| **$\upsilon_{as}$(BO) in $BO_3$** | 1383 | 1383 | 1383 | 1383 | 1384 |

**Table 4:** Compositions of the samples prepared within the system.

| Sample | X | 0.95-x |
|---|---|---|
| BA1 | 0.30 | 0.65 |
| BA2 | 0.35 | 0.60 |
| BA3 | 0.40 | 0.55 |
| BA4 | 0.45 | 0.50 |
| BA5 | 0.50 | 0.45 |

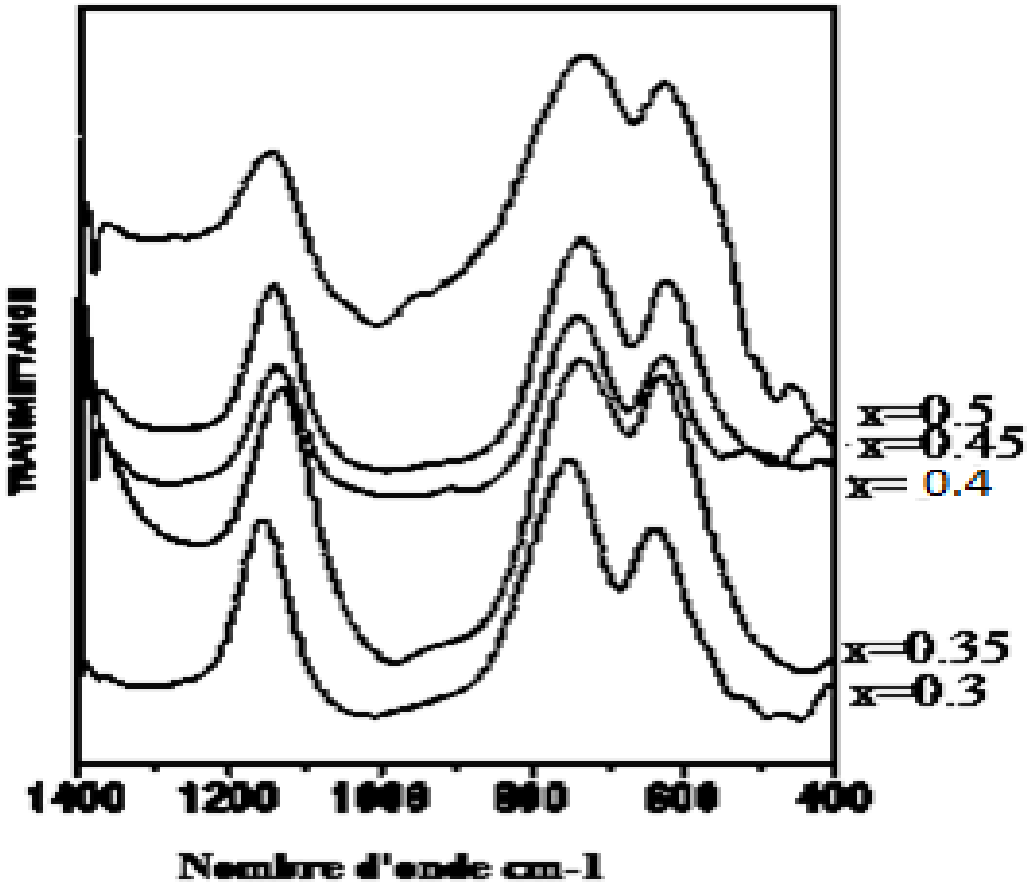


**Figure15:** Infrared spectra of the compositions $(0.95\text{-}x)Bi_2O_3\text{-}xB_2O_3\text{-}(0{,}025P_2O_5\text{-}0{,}025Nb_2O_5)$

**Table 5:** Infrared frequency assignments of the glasses of the compositions $(0.95\text{-}x)Bi_2O_3\text{-}xB_2O_3\text{-}(0{,}025\ P_2O_5\text{-}0{,}025\ Nb_2O_5)$

| **N° of Sample** | **$BA_1$** | **$BA_2$** | **$BA_3$** | **$BA_4$** | **$BA_5$** |
|---|---|---|---|---|---|
| **Composition** | x=0.30 | x=0.35 | x=0.4 | x=0.45 | x=0.5 |
| **skeletons Bi-O-Bi**<br>**Or skeletons B-O-Bi**<br>**Or skeletons B-O-B** | 413 | 434<br>468<br>484 | 410<br>446<br>482 | 403<br>457<br>510 | 426<br>454<br>496 |
| **Métaborates$\upsilon_{a\ B\text{-}O\text{-}Nb}$** | 636 | 657 | 669 | 672 | 675 |
| **Métaborates$\upsilon_{a\ B\text{-}O\text{-}P}$** | 692 | 692 | 693 | 693 | 695 |
| **orthophosphates** | 695 | 721 | ------- | ------- | -------- |
| **Boroxol** | 905 | 860 | 885 | -------- | |
| **orthoborates $BO_3$** | 997 | 965 | 961 | 953 | 904 |
| **BO ($BO^{4-}$)** | 1025 | 1034 | 1026 | 1030 | 1048 |
| **Pyroborates B-$O^-$** | 1221 | 1227 | 1230 | 1238 | 1241 |
| **$\upsilon_{as}$(BO) dans $BO_3$** | 1316 | 1383 | 1383 | 1383 | 1384 |

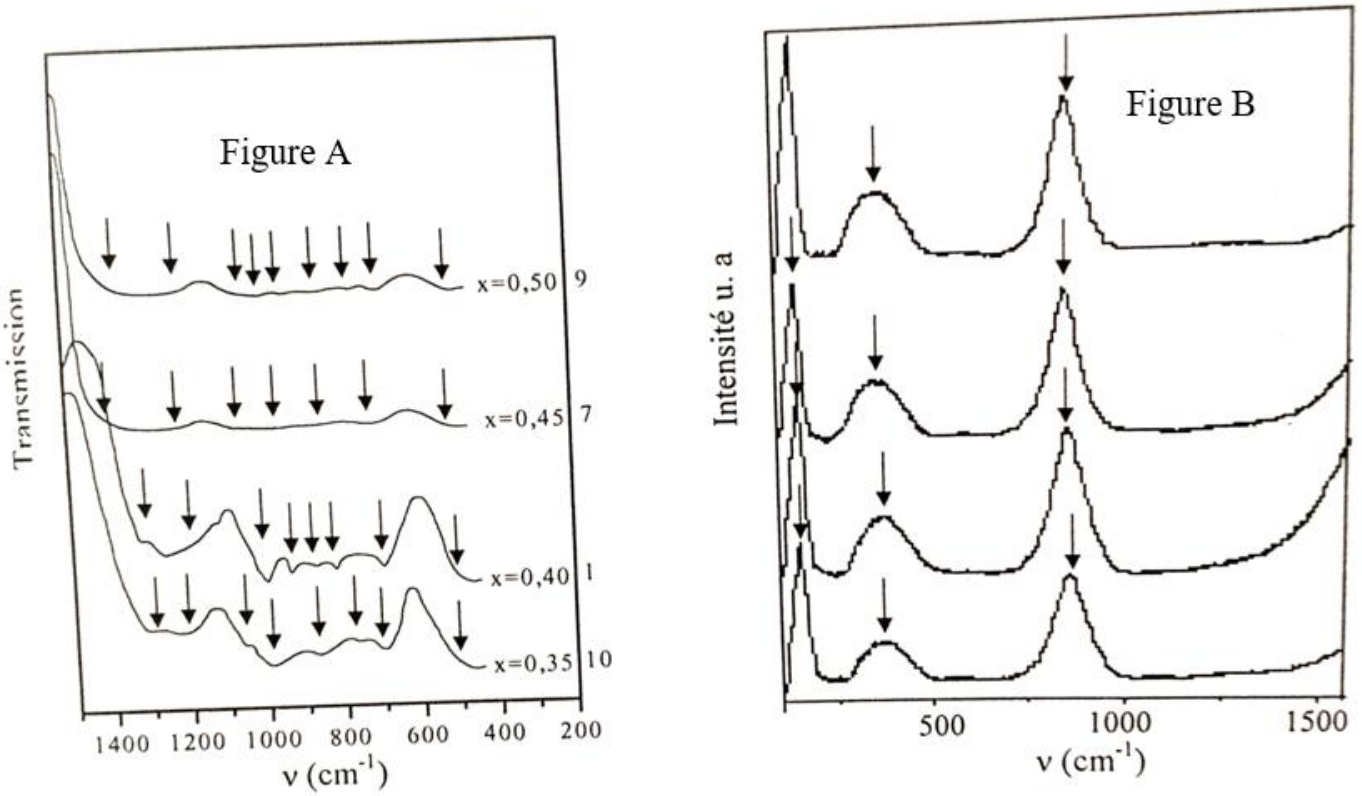


**Figure 16:** Raman (B) and infrared (A) spectra of glasses with different compositions$(0,90\text{-}x)Bi_2O_3\text{-}xB_2O_3\text{-}0,1V_2O_5$

**Table 6:** Infrared spectra of glasses with different compositions $(0,90\text{-}x)Bi_2O_3\text{-}xB_2O_3\text{-}0,1V_2O_5$

| N° of Sample | 1 | | 2 | | 3 | | 4 | |
|---|---|---|---|---|---|---|---|---|
| Composition | x=0.35 | | x=0.4 | | x=0.45 | | x=0.5 | |
| Spectroscopy | IR | Ra | IR | Ra | IR | Ra | IR | Ra |
| Network vibration | | 160 | | 160 | | 160 | | 160 |
| Skeleton B-O-B | | 370 | | 371 | | 360 | | 360 |
| Skeleton Bi-O-B | 482 | | 481 | | | | | |
| Skeleton Bi-O-B | | | | | 520 | | 511 | |
| Méthaborate$\upsilon_s$BO V | 698 | | 688 | 560 | 710 | | 684 | 562 |
| -orthoborate $BO_3$ | 856 | 854 | 868 | 856 | 830 | 858 | 834 | 863 |
| -PyroboratesB-$O^-$ | 1210 | | 1250 | | 1270 | | 1280 | |
| -$\upsilon_{as}$(BO)dans $BO_3$ | 1306 | | 1317 | | | | | |

**Table 7:** Compositions of the samples prepared in the system $(0,90\text{-}x)Bi_2O_3\text{-}xB_2O_3\text{-}(0,05V_2O_5\text{-}0,05Nb_2O_5)$

| Sample | x | 0.90-x |
|---|---|---|
| NA1 | 0.3 | 0.6 |
| NA2 | 0.35 | 0.55 |
| NA3 | 0.4 | 0.5 |
| NA4 | 0.45 | 0.45 |
| NA5 | 0.5 | 0.4 |

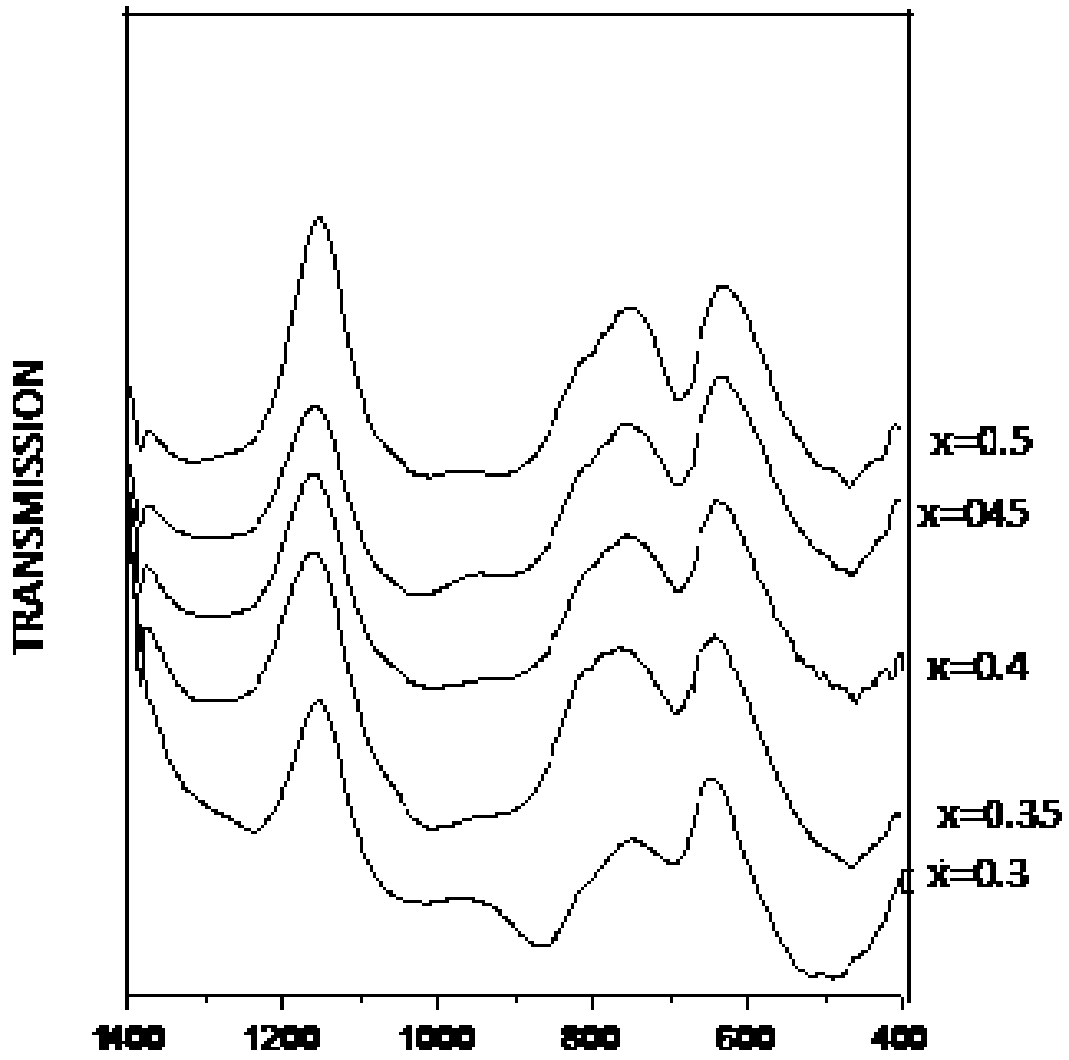


**Figure 17:** Infrared spectra of $(0.90\text{-}x)Bi_2O_3\text{-}xB_2O_3\text{-}(0.05V_2O_5\text{-}0.05Nb_2O_5)$

**Table 8:** Infrared frequency assignments of the glasses of the compositions $(0,90\text{-}x)Bi_2O_3\text{-}xB_2O_3\text{-}(0,05V_2O_5\text{-}0,05Nb_2O_5)$

| N°.Echantillon | | NA1 | NA2 | NA3 | NA4 | NA5 |
|---|---|---|---|---|---|---|
| Composition | | X=0,30 | X=0,35 | X=0.4 | X=0.45 | X=0.5 |
| Attributions | δskeleton δ (B-O-B)<br>or δ (Bi-O-Bi)<br>or δ (Bi-O-B) | ------<br>475<br>507 | -----<br>469<br>494 | ------<br>470<br>---------- | 486<br>------<br>---------- | 466<br>-------<br>-------- |
| | Méthaborates $\upsilon_s$(B-O-Nb) | 668 | 669 | ---------- | --------- | --------- |
| | Pyrovanadate group $V_2O_7^{4-}$ | 777 | 778 | ---------- | --------- | ------ |
| | Group $VO_4$ | 798 | 799 | 796 | ------- | ------- |
| | metaborates$\upsilon_s$(B-O-V) | 698 | 701 | 698 | 697 | 693 |
| | orthovanadate | 894 | 907 | 910 | ------ | ------ |
| | orthoborate ($BO_3$) | 1032<br>1008 | 1030<br>1008 | 1028 | 1030 | 1033 |
| | pyroborates B-$O^-$ | 1235 | 1310 | 1311 | 1324 | ------- |
| | $\nu_{as}$(BO) dans $BO_3$ | 1382 | 1381 | 1382 | 1384 | 1382 |

**Table 9:**Compositions prepared within the system $(0,95\text{-}x)Bi_2O_3\text{-}xB_2O_3\text{-}(0,025Ta_2O_5\text{-}0,025Nb_2O_5)$

| Sample | 0.95-x | x |
|---|---|---|
| $A_1$ | 0.65 | 0.3 |
| $A_2$ | 0.6 | 0.35 |
| $A_3$ | 0.55 | 0.4 |
| $A_4$ | 0.5 | 0.45 |
| $A_5$ | 0.45 | 0.5 |

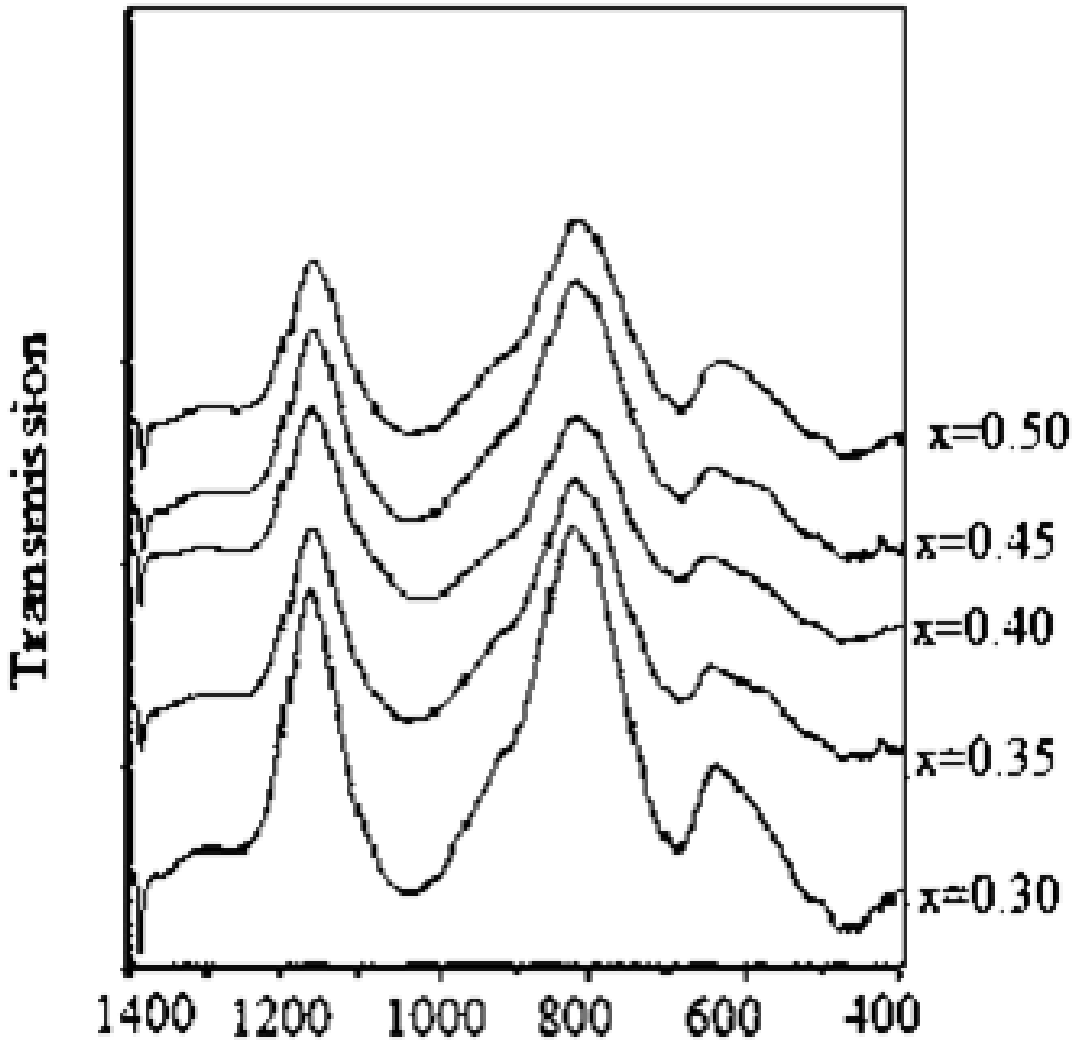


**Figure 18:** Infrared spectra of glasses(0.95-x)Bi2O3-xB2O3-(0.025Ta2O5-0.025Nb2O5)

**Table 10:** Infrared frequency allocations for glass compositions $(0,95-x)Bi_2O_3-xB_2O_3-(0,025Ta_2O_5-0,025Nb_2O_5)$

| **N° of sample** | | $A_1$ | $A_2$ | $A_3$ | $A_4$ | $A_5$ |
|---|---|---|---|---|---|---|
| **Composition** | | x=0.30 | x=0.35 | x=0.4 | x=0.45 | x=0.5 |
| **Attributions** | **υ skeleton (Bi-O-Bi)** | 482 | 480 | 473 | 469 | 461 |
| | **υ skeleton (B-O-Bi)** | ---- | 426 | 427 | 438 | 449 |
| | **υ skeleton (B-O-B)** | 551 | 523 | 510 | ---- | ----- |
| | **υ (Nb-O)** | 670 | 668 | 669 | 690 | 688 |
| | **υ (Nb-O-Nb)** | 637 | 636 | 620 | 625 | ---- |
| | **υ (Ta-O-Nb)** | ---- | 507 | 542 | 588 | 593 |
| | **υ (Ta-O)** | ---- | ---- | ---- | ---- | ---- |
| | **Boroxol** | ---- | ---- | ---- | ---- | ---- |
| | **orthoborates $BO_3$** | ---- | ---- | ---- | ---- | ---- |
| | **$\upsilon_s$ BO ($BO^{4-}$)** | ---- | 1002 | 1016 | 1034 | 1036 |
| | **Pyroborates B-$O^-$** | 1216 | 1243 | 1244 | 1249 | 1250 |
| | **$\upsilon_{as}$(BO) dans $BO_3$** | 1316 | ---- | ---- | ---- | ---- |

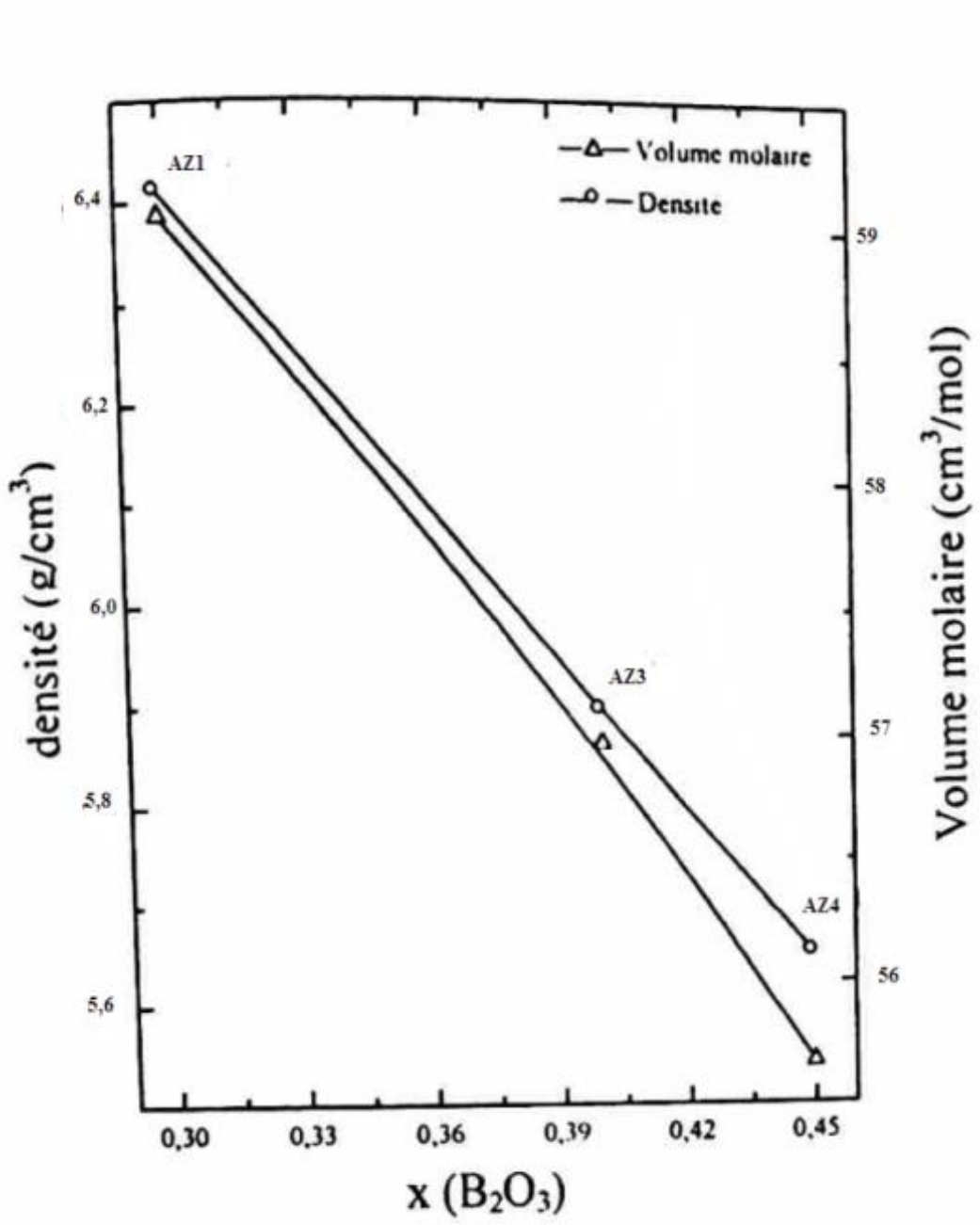


**Figure 19:** variation of density and molar volume of glasses of different compositions (0,90-x) $Bi_2O_3$-x$B_2O_3$-(0.05$P_2O_5$-0.05$Nb_2O_5$)

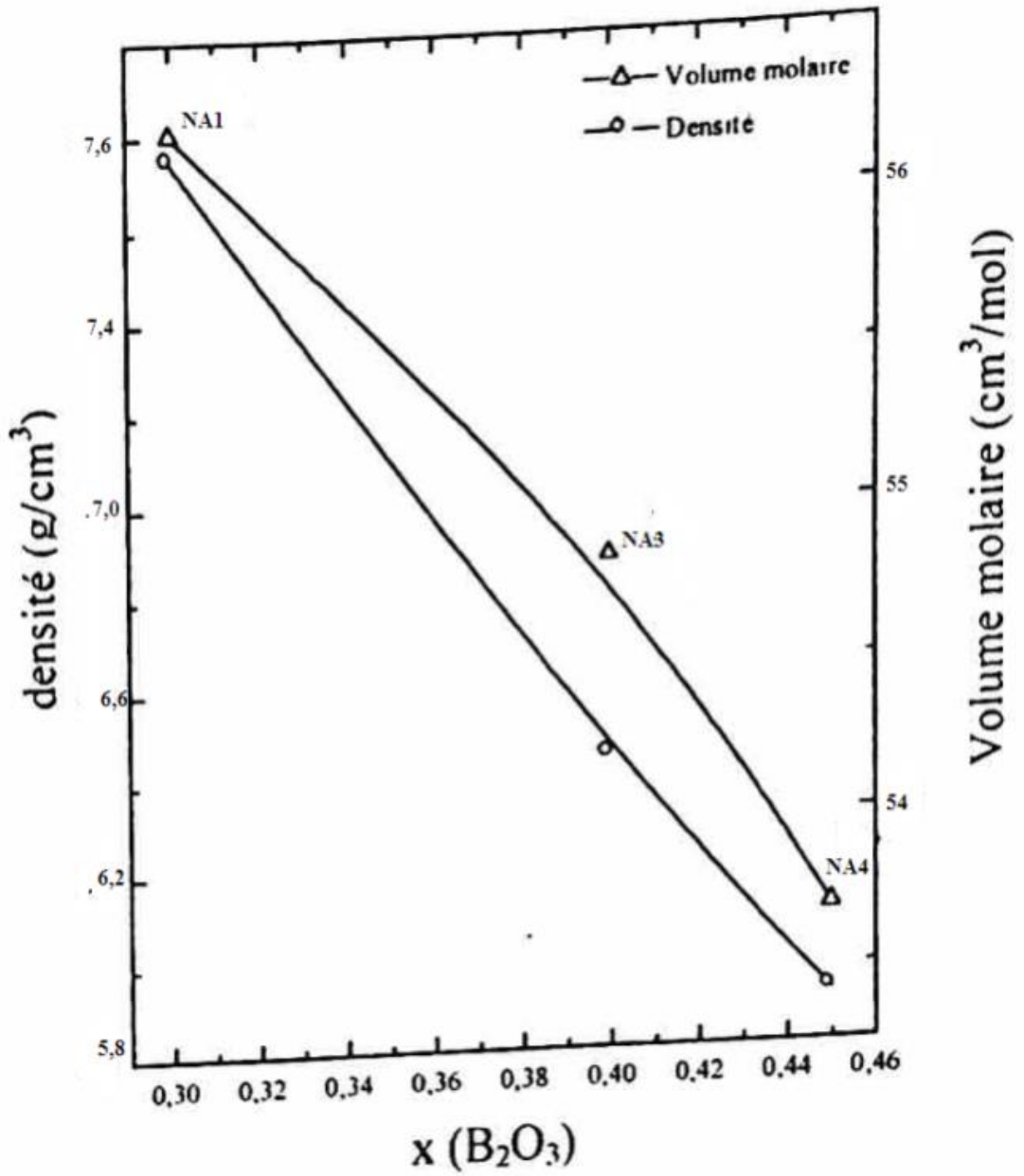


**Figure 20:** variation of the density and molar volume of glasses of different compositions(0,90-x) $Bi_2O_3$-x$B_2O_3$-(0.05$V_2O_5$-0.05$Nb_2O_5$)

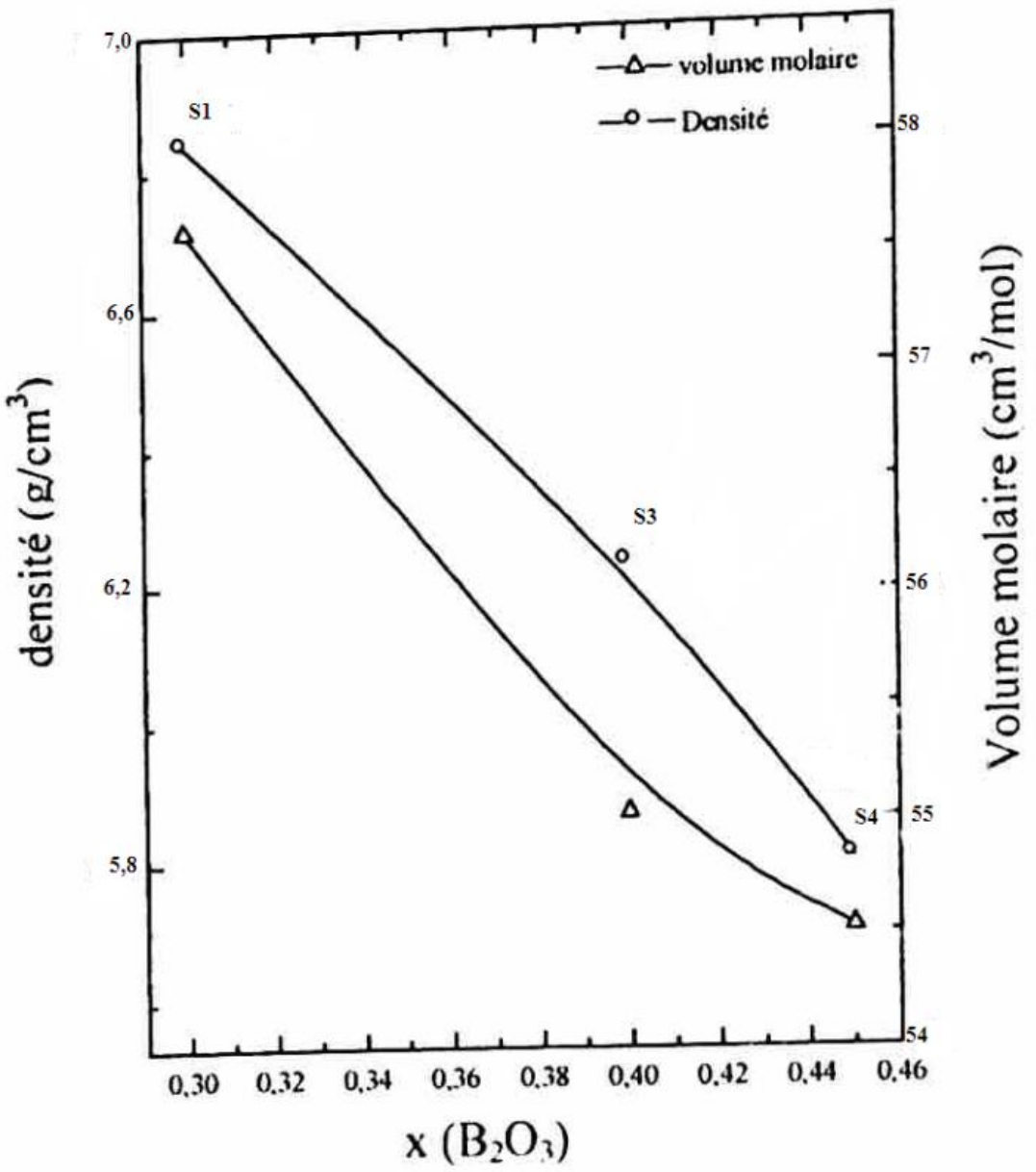


**Figure 21:** variation of density and molar volume of glasses with different compositions(0,90-x) $Bi_2O_3$-x$B_2O_3$-(0.05$Ta_2O_5$-0.05$Nb_2O_5$)

## 4. Conclusions

The glasses of the compositions(0.90-x) $Bi_2O_3$-x$B_2O_3$-0,1$M_2O_5$,(0.90-x)$Bi_2O_3$-x$B_2O_3$-(0,5$M_2O_5$-0,5$Nb_2O_5$)Et(0.95-x)$Bi_2O_3$-x$B_2O_3$-(0,025 $M_2O_5$-0,025$Nb_2O_5$)Such that M=P, V or Ta ;A comparative study was made to evaluate the differences that exist within the glassy framework in each area. We observe a significant difference between the samples containing niobium and phosphorus and those with only phosphorus, indeed the line at 1050 $cm^{-1}$ noted in the study of bismuth borophosphates, disappears completely, on the other hand another line at 880 $cm^{-1}$ appears for the compositions of glassy domains.We recall that the 1050 $cm^{-1}$ line is attributed to υ($PO_2$) in the $MB_2$ and $MB_2$' groups, its disappearance probably implies the non-existence of these groups for the compositions of the domain with niobium and phosphorus consequently the latter should not participate in the glassy framework, but is found in the form of an independent $PO_4$ group. For the samples containing niobium and vanadium, the spectra confirm the non-existence of the band at 1050 $cm^{-1}$ and the presence of the band at 880 $cm^{-1}$ for all compositions. The hypothesis of the presence of $M_vB_2$ and $M_vB_2$' groups seems to us the most probable. The spectra show the presence of metaborates and diborates in the glassy frameworks; bands at 1320 cm-1 and 1220 cm-1 respectively. However, the bands with boron in the four coordinate are more intense in the case of compositions containing only vanadium.We also notice a significant difference between the samples containing vanadium and niobium and those with phosphorus and niobium and those with tantalum and niobium which allows to draw :

The increase of $Nb_2O_5$ and $P_2O_5$ contents in the $Bi_2O_3$-$B_2O_3$-($Nb_2O_5$-$P_2O_5$) system leads to :
- The decrease of the intensity of the band corresponding to the B-O-P groups.
- The disappearance of the bands Bi-O-B.
- The disappearance of the bands assigned to the orthoborate and orthophosphate groups.
- We also find that there is a displacement of the band corresponding to the pyroborates BO- towards the high frequencies.

This explains the accentuation of the depolymerization of the glassy framework.

The increase of $Nb_2O_5$ and $V_2O_5$ contents in the $Bi_2O_3$-$B_2O_3$-($Nb_2O_5$-$V_2O_5$) system leads to :
- The disappearance of the band of $V_2O_7^{4-}$ and $VO_4$ groups.
- The increase of the intensity of the B-O-V band.
- A decrease of the band located between 800 $cm^{-1}$ and 1100 $cm^{-1}$.

The increase of $Ta_2O_5$ and $Nb_2O_5$ contents in the $Bi_2O_3$-$B_2O_3$-($Ta_2O_5$-$Nb_2O_5$) system leads to :
-A disappearance of the band corresponding to the groups orthoborate groups $BO_3$.
-A disappearance of the inversion of υas(BO) in $BO_3$.

The bands of the glasses containing phosphorus and niobium and those with vanadium and niobium evolve in the same way in the case of the substitution of bismuth by boron, but the intensities of these bands increase in the samples containing vanadium

The bands of the glasses containing tantalum and niobium and those with phosphorus and niobium evolve in the same way in the case of the substitution of bismuth by boron, but the intensities of these bands increase in the samples containing phosphorus.

## References


[1] Jr, P. D.Myers, T. E. Alam, R.Kamal, D. Y. Goswami, E. Stefanakos.(2016). Nitrate salts doped with CuO nanoparticles for thermal energy storage with improved heat transfer. Applied Energy. 165: 225-233.

[2] A. G. Roca, L. Gutiérrez, H. Gavilán, M. E. Brollo, S.Veintemillas-Verdaguer, M. del Puerto Morales, (2019). Design strategies for shape-controlled magnetic iron oxide nanoparticles. Advanced drug delivery reviews.138:68-104.

[3] S.K. Barik, A.Senapati, , S. Balakrishnan, K.Ananthasivan. ( 2022). Synthesis and characterization of rare-earth doped aluminium phosphate glasses. Progress in Nuclear Energy, 152:104372.

[4] A.Kishioka. (1978).Transition metals in organic synthesis: Annual survey covering the year 1978. Bull. Chem. Soc. Japon .51:2552.

[5] Y.Fujita, Y. Kawasaki, T. Inaoka, T.Kimura, A. Sakuda, M. Tatsumisago, A. Hayashi. (2021). Amorphous Li2O–LiI solid electrolytes compatible to Li metal. Electrochemistry.21:00049..

[6] G. P. Johari, E.Tombari. (2022). On the decrease of entropy on cooling polymer melts and an orientationally-disordered crystal. Thermochimica Acta.711:179186.

[7] J.Zarzycki. (1982). The glasses and the vitreous state. Masson.

[8] C.Lucat, G. Campt, J. Claverie, J. Portier, J. Reau, P. Hagenmuller. (1976). Sur de nouveaux conducteurs anioniques de hautes performances. Mater. Res. Bull. 11:167.

[9] M . El Faydy, M .Galai, R .Touir, A .El Assyry, M .Ebn Touhami, B .Benali, B .Lakhrissi, A.Zarrouk .( 2016).Experimental and theoretical studies for steel XC38 corrosion inhibition in 1 M HCl by N-(8-hydroxyquinolin-5-yl)-methyl) –N-phenylacetamide. J Mater Environ Sci;7(4)1406-16.

[10] M. Galai, M.El Faydy, Y.El Kacimi, K.Dahmani, K.Alaoui, R. Touir, , B .Lakhrissi , M. Ebn Touhami.(2017). Synthesis, characterization and anti-corrosion properties of novel quinolinol on C-steel in a molar hydrochloric acid solution. Port Electrochim Acta, 35(4) 233-251.

[11] M . Galai, J .Ouassir, M .Ebn Touhami, H. Nassali, H .Benqlilou, T .Belhaj, K .Berrami, I .Mansouri, B .Oauki.( 2017). α-Brass and (α + β) brass degradation processes in azrou soil

medium used in plumbing devices. J Bio Tribo Corros.3(3).

[12] L .Kadiri, M .Galai, M .Ouakki, Y .Essaadaoui, A .Ouass, M .Cherkaoui, E. H.Rifi, A .Lebkiri.(2018) Coriandrum sativum.L seeds extract as a novel green corrosion inhibitor for mild steel in 1.0 M hydrochloric and 0.5 M sulfuric solutions. Anal Bioanalytical Electrochem .10(2) 249-68.

[13] M .Galai, M .Rbaa, M .Ouakki, AS.Abousalem, E .Ech-chihbi, K .Dahmani, N .Dkhireche, B Lakhrissi, M .Ebn Touhami.(2020) .Chemically functionalized of 8-hydroxyquinoline derivatives as efficient corrosion inhibition for steel in 1.0 M HCl solution: Experimental and theoretical studies. Surf Interfaces .21.

[14] A. Nimour, M. Belfaquir, T. Guedira, J. L. Rehspringer, (2013). Étude des propriétés électriques des phases des systèmes $Bi_2O_3$-$P_2O_5$-MO (M= Ba, Ca). Bulletin de la Société Royale des Sciences de Liège.

[15] A.Borowska-Centkowska, X.Liu, M.Holdynski, M. Malys, S. Hull, F. Krok, I. Abrahams.(2014). Conductivity in lead substituted bismuth yttrate fluorites. Solid State Ionics, 254: 59-64.

[16] M. Imran, A. B.Yousaf, M.Farooq, P. Kasak. (2022). Enhancement of visible light-driven hydrogen production over zinc cadmium sulfide nanoparticles anchored on BiVO4 nanorods. International Journal of Hydrogen Energy, 47(13)8327-8337.

[17] A. Elbadaoui, M.Galai, M.Cherkaoui, T. Guedira, .(2016). Preparation and characterization of a vitreous phase and application as a corrosion inhibitor in acidic medium. Der Pharma Chemica, 8(6).

[18] J.Chen, W.Fang, Y. Tang , L.Fang. (2021). Effects of LiF addition on the densification and microwave dielectric properties of LiInO2 ceramics. Ceramics International, 47(20) 28960-28967.

[19] J.Zhang, W. Wang, T. Wang, L.Jiang, N. Wang, , Y. Dai, Y. Qi, (2021). Atomic-scale analysis of the interface structure and lattice mismatch relaxation of Bi2Sr2CaCu2O8+ δ/SrTiO3 heterostructure. Ceramics International, 47(6) 8722-8727.

[20] A.Elbadaoui, M. Galai, S.Ferraa, H. Barebita, M.Cherkaoui, T.Guedira. (2019). A new family of borated glasses as a corrosion inhibitor for carbon steel in acidic medium (1.0 M HCl). Anal. Bioanal. Electrochem., 11(1)19-37..

[21] M. BELFAQUIR, T. GUEDIRA, S. M. D. ELYOUBI, J. L. REHSPRINGER.(2013). Structural study of borate glasses of the system $Bi_2O_3$-$B_2O_3$-$P_2O_5$. ScienceLib. 5:130302.

[22] A.Elbadaoui, , M.Galai , S. Ferraa, H. Barebita, , M. Cherkaoui, T. Guedira, (2019). Effect of bismuth and bore content in glass system inhibitor on the corrosion behavior of mild steel in 1M hydrochloric acid solution. Mediterranean Journal of Chemistry, 8(4) 328-337.

[23] A. Elbadaoui, M.Galai, S. Ferraa, H. Barebita, M. Cherkaoui, T. Guedira. (2022). A new family of borated glasses as a corrosion inhibitor for steel in 1.0 M hydrochloric acid: synthesis and cauterization studies. Int. J. Corros. Scale Inhib, 11(2) 666-685.

[24] Baia,R.Stefan, W. Kiefer,J.Popp and S.Simon,. (2002). Structural investigations of copper doped B2O3–Bi2O3 glasses with high bismuth oxide content.Journal of non-crystalline 303.

[25] S.Ferraa, H.Barebita, M. Moutataouia, A.Nimour, A.Elbadaoui, B. Baach, T.Guedira. (2021). Effect of barium oxide on structural features and thermal properties ofvanadium phosphate glasses. Chemical Physics Letters, 765: 138304..

[26] H.Barebita, S. Ferraa, M. Moutataouia, B. Baach, A.Elbadaoui, A.Nimour, T. Guedira. (2020). Structural investigation of $Bi_2O_3$-$P_2O_5$-$B_2O_3$-$V_2O_5$ quaternary glass system by Raman, FTIR and thermal analysis. Chemical Physics Letters. 760: 138031..

[27] O.Barzali, A. Ben Ali, H. Ait Ahsaine, Y.Kerroum, M. Saadi. (2022). Synthesis, structural and the corrosion inhibition of phosphate-based xPbO–$yB_2O_3$–$zP_2O_5$ glass for C35 steel in acidic media. Nanotechnology for Environmental Engineering. 7(1) 277-287.

[28] K. I. Chatzipanagis, N. S. Tagiara, E. I. Kamitsos, , N. Barrow, I.Slagle, R. Wilson, S. Feller. (2022). Structure of lead borate glasses by Raman, 11B MAS, and 207Pb NMR spectroscopies. Journal of Non-Crystalline Solids, 589: 121660.

[29] Y. Xia, W. Zhu, J. Sen, S. Sen. (2020). Observation of polymer-like flow mechanism in a short-chain phosphate glass-forming liquid. The Journal of Chemical Physics, 152(4) 044502.

[30] J.Yiven, C.Xiangshengt,H.Xihuai. (1989). Raman studies of lithium borophosphate glasses. Journal of Non-Crystalline Solids 112: 147.

[31] B.B.Meera,A.K.Sppd,N.chandradhas and J.Ramakrishna.(1990). Raman study of lead borate glasses. Journal of Non-Crystalline Solids 126:224.

[32] G.D. Chryssikos,E.I.Kamitos and W.M.Risen Jr. (1987). A Raman investigation of cadmium borate and borogermanate glasses. Journal of Non-Crystalline Solids 93:155.

[33] A. M. Al-Syadi. (2021). Electrochemical performance of Na2O–Li2O–P2S5–V2S5 glass–ceramic nanocomposites as electrodes for supercapacitors. Applied Physics A. 127(10) 1-11.

[34] J. Masse, H. Szymanowski, O. Zabeida, A. Amassian, J.E. Klemberg- Sapieha, L. Martinu. (2006). Stability and effect of annealing on the opticalproperties of plasma-deposited $Ta_2O_5$ and $Nb_2O_5$ films. Thin Solid Films. 515:1674–1682.

[35] H. Y. Kim, P.Viswanathamurthi, N.Bhattarai, D. R. Lee. (2003). Preparation and morphology of niobium oxide fibers. Reviews on Advanced Materials Science, 5(3) 224-227.

[36] A. M. R. Galletti, C. Antonetti, V. De Luise, M.. Martinelli, (2012). A sustainable process for the production of γ-valerolactone by hydrogenation of biomass-derived levulinic acid. Green Chemistry, 14(3) 688-694.

[37] M. S.Mansha, , T. Iqbal. (2022). Experimental and theoretical study of novel rGO/AgVO3 nano-hetrostructures for their application as efficient photocatalyst. Optical Materials. 131:112591.